**Proceedings of the Canadian Society for Mechanical Engineering International Congress**
**32nd Annual Conference of the Computational Fluid Dynamics Society of Canada**
**Canadian Society of Rheology Symposium**
**CSME-CFDSC-CSR 2025**
**May 25–28, 2025, Montréal, Québec, Canada**

# Numerical and Experimental Investigation of Snow Accumulation on Surfaces

Kiran P. Keshavan[1*], Mohammad S. M. Ghareghani[1], Farimah Hosseinnouri[1], Martin Agelin-Chaab[1], Horia Hangan[1]

[1] Department of Mechanical and Manufacturing Engineering,
Ontario Tech University, Oshawa, L1G 0C5, Canada
kiran.purushothamakeshavan@ontariotechu.net

***Abstract* —** Snow accumulation on surfaces is a significant cause of contamination and can obstruct visibility on vehicles; this can pose a significant safety hazard. To investigate snow adhesion, experiments were conducted in a controlled environment with no wind using artificial snow from a snow gun at sub-zero temperatures. Surfaces at different angles of incline were tested across a range of temperatures to observe snow accumulation. Particle data, including particle size and fall velocity, was captured using a disdrometer. In addition, the numerical modelling of the experiments has been conducted. Adhesion criteria defined in terms of critical velocity and critical particle radius for rolling and sliding were imposed on the collected data. Further numerical analysis of the results revealed that the tendency of snow to adhere to surfaces rises with an increase in temperature values. Non-dimensional numbers that quantify the observed phenomena were compared with experimental results from the climatic chamber. Additionally, the numerical model revealed an inverse relationship between the surface incline angle and the predicted number of particles adhering upon impact.

***Keywords- DEM, JKR, Adhesion, Cohesion, sticking efficiency***

## I. INTRODUCTION

Recent advancements in snow accumulation research have enhanced our understanding of accretion dynamics on moving surfaces under varying environmental conditions. Notably, recent studies have developed predictive models for snow accretion on autonomous vehicles, integrating key factors such as ambient temperature, relative humidity, and wind speed to improve accuracy and reliability. These models are designed to enhance the operational safety and reliability of autonomous systems in snow-prone environments [1] [2]. The definition of snow has been a highly debatable topic for years, illustrations of various morphologies of naturally occurring and artificial snow have been discussed [3]. Moreover, the degree of similarity between artificial snow and natural snow varies based on the production method. Compared to natural fresh snow, artificial snow is denser due to its compact structure for snow produced by a snow gun [4]. The structural complexity of natural or artificial snow needs to be studied to model an accurate adhesion model which explains snow builds up under different climatic conditions.

Studies manipulate variables such as wind speed and direction to analyze their influence on snow distribution patterns, providing valuable insights into the aerodynamic effects on snow accumulation [5] [6]. Snow's interaction with fluid media further complicates the adhesion or cohesion studies. To simplify this complex phenomenon and better understanding the fundamental mechanisms of snow deposition, experiments with artificial snow at a climatic chamber with no wind have been conducted at the ACE (Automotive Centre of Excellence) facility at Ontario Tech University. Experimental data in terms of particle size distribution, particle fall velocity, accumulation height, resting density, effect of incline, and temperature effects were recorded from these tests.

For dry adhesion, interparticle forces, such as van der Waals forces, play a crucial role in adhesion as well as in the formation and disintegration of particle agglomerates. These forces are integrated into an in-house numerical code based on the discrete Element Method (DEM) theory, which predicts the nature of interaction these individual particles have with a surface or with particles of a similar kind as discussed in [7]. In reference [8], particle impingement on surfaces has been studied with much detail to predict particle rebound and breakage, but particle dynamics post impact is not the focus of the current study. In this study, the Johnson-Kendall-Roberts (JKR) model which accounts for adhesive elastic deformation at contact is employed to characterize particle-particle & particle-wall interactions. Like in [7], this work has further numerically investigated particle agglomerate impact on surfaces using JKR theory to establish an adhesion criterion that predicts a number of particles that may potentially stick to a surface. More specifically, critical velocity for particle agglomerate adhesion & the calculation of sliding friction force ($F_s$) and rolling moments ($M_c$) give an approximate critical sliding and rolling radius for varying angles of surface incline. The porosity of snow is assumed to be 50% in

[7], but in this study the effects of porosity of particle agglomerate has not been considered. The porosity of artificial snow at the individual particulate level has been neglected, as its effects are more significant at the microscale. Since this study focuses on particle-level adhesion rather than the internal microstructure of snow agglomerates, the porosity of snow has been ignored. To numerically model snow accumulation on varying inclines, numerical coefficients like sticking efficiency, which has been introduced by Makkonen [9] has been utilized. This model for accretion has been established specifically for overhead transmission lines, but in this work, this theory has been extended to flat surfaces at different angles of inclination. Comparing the normalized numerical sticking efficiency with the normalized experimentally obtained sticking efficiency gives an insight into how adhesive snow can get over a range of temperatures.

## II. Methodology

### A. Experimental

Multiple tests at the Large Climatic Chamber in the ACE facility were conducted to study the properties of snow. The experimental setup is shown in Fig 1. As part of the experiments the accumulation of snow on surfaces set at three different angles: 0°, 30°, and 40° (Fig. 1a - 1c) has been studied. These surfaces were placed at a distance of 4 meters from the snow gun. The aim was to observe how snow accumulated on each surface under various temperature conditions ($-15℃$, $-10℃$ & $-5℃$). From the tests, the following properties of artificial snow were recorded: Accumulation height, particle fall velocity, particle size distribution, resting density, and temperature of the climatic chamber over the duration of each test. A snow gun, positioned at a fixed angle, generated machine-made snow under stable and controlled temperature conditions. Since there are no wind effects except drag force on the particle, the artificial snow projected toward the facility's roof allowed the particles to descend vertically onto the designated test. Over a 20-minute period, snow accumulation was monitored across different surface inclinations. Data like fall velocity and particle diameter has been recorded for different temperature values, a visual representation of this can be found in Fig. 4.

### B. Numerical

In this study, a custom code in MATLAB has been utilized to address 2 critical questions from the experiments: - The estimation of the cohesiveness of snow at varying temperature values in a controlled environment and the impact of surface inclination on the adhesion between particles and the wall (as well as the cohesion between particles). The prediction of the primary mechanism governing whether a single particle sticks or bounces uses the normal impact interaction model. With this, sliding force and torque contributions of particles upon contact with a surface have been studied using critical sliding force and rolling moment criteria, which is explained in detail in Section III below. The flowchart detailed in Fig. 2 gives the procedure for predictive modeling for particle adhesion study.

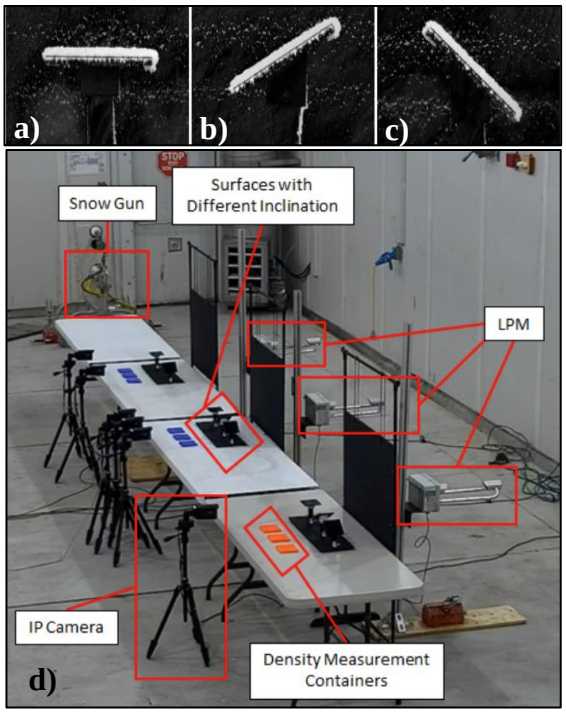


*Figure 1: Accumulation of snow on inclined surfaces and experimental setup*

## III. Theory

To model cohesion or adhesion, an attractive force component has been incorporated in numerical analysis. These forces are dependent on material properties [7] which are based on the data obtained from references [10] and [11]. Values for density, Young's modulus, and Poisson's ratio were analyzed to ensure an accurate characterization of the material property for snow. The surface used for snow accumulation is polymethyl methacrylate (PMMA) or plexiglass, and the material properties, including Young's modulus and Poisson's ratio, were determined as follows [12]: $E_{acrylic}=3.1\times10^9$ Pa & $\nu_{acrylic}=0.3$ [12].

Numerous existing contact models, including the JKR, DMT, linear cohesion model, and capillary force models, are based on principles of elastic collision [13]. The JKR and DMT adhesion models are among the most widely used contact models for describing dry particle adhesion. To determine whether to apply the JKR or DMT models, [14] & [15] talk about a critical value for the dimensionless Tabor number $\lambda_T$.

$$\lambda_T = \left(\frac{RW^2}{E^2\delta^3}\right)^{\frac{1}{3}} \quad (1)$$

The contact deformation used for the Tabor number is critical [14]. The equilibrium separation distance $\delta$ is 1.65 Å [16]. R and E are the effective radius and effective Young's modulus [7].

Olsson [14] considers a threshold of $\lambda_T > 3$ for the use of the JKR adhesion model but according to [15], for $\lambda_T > 5$, the JKR model is appropriate. Moreover, both [14] & [15] suggest that DMT is more suitable for instances where $\lambda_T < 0.1$. To calculate the Tabor number, normal overlap at equilibrium

contact has been considered, and since, for the present case, the value for $\lambda_T > 5$, therefore, the JKR adhesive contact model has been chosen as an appropriate adhesion model for this study.

According to the JKR model, a finite adhesion force $F_a$ is required to separate a spherical object from a flat surface. This is expressed as follows [17]

$$F_a = \frac{3}{2}\pi W R \tag{2}$$

Also, the work of cohesion needed to detach the spheres from contact is given by [15],

$$W_c = 7.09 \times \left(\frac{W^5 R^4}{E^2}\right)^{\frac{1}{3}} \tag{3}$$

When two dissimilar media, 1 and 2, come into contact, the work of adhesion between these two media would be $W_{12}$. When particles of the same material are in contact with each other, then, the work of cohesion can be symbolized as: $W_{11} = 2\gamma_{11}$. It is important to note that adhesive work and cohesive work are distinct. The surface energies of the materials in contact are represented by $\gamma_1$& $\gamma_2$. $\gamma_{12}$ is the interfacial energy which represents two distinct quantities. One way of calculating the work of adhesion is by using Dupre's equation [18],

$$\gamma_{12} = \gamma_1 + \gamma_2 - W_{12} \tag{4}$$

According to Fowkes [19], molecular interactions can be categorized into two types: metallic or hydrogen bonds, which depend on the chemical properties of the particles ($\gamma^{p}_{material}$) which mostly occur due to ionic or hydrogen bonds, and London dispersion forces ($\gamma^{d}_{material}$). These forces are universal and occur between particles of different chemical compositions [20]. Of these, the latter occurs mostly because of dipole interactions between atoms and molecules across the interface. This can be expressed mathematically as follows:

$$\gamma_{material} = \gamma^{d}_{material} + \gamma^{p}_{material} \tag{5}$$

As stated in [16], [21] & [22] the surface energy of ice is primarily dispersive rather than polar. The same goes for polymethyl methacrylate (PMMA), also known as Plexiglas [23] & [24].

There are many methods of calculating surface energies of materials, but in [24] the surface energies for PMMA have been calculated using various methods.

Among these methods, the acid-base approach has been concluded as the most accurate for measuring surface energies. This interfacial surface energy between 2 dissimilar materials can be calculated using Fowke's theory[19].

$$\gamma_{12} = \gamma_1 + \gamma_2 - 2\sqrt{\gamma_1^d \gamma_2^d} \tag{6}$$

This process involves two key interactions: adhesion and cohesion. ($W_{12}$) of 0.116 J/m². Cohesion occurs between successive ice/ snow layers, with a work of cohesion ($W_{11}$) of 0.212 J/m² between the subsequent layers of snow. For particles that make normal contact with a surface (or another particle) and if the velocity (at contact) equals to zero, it means that the

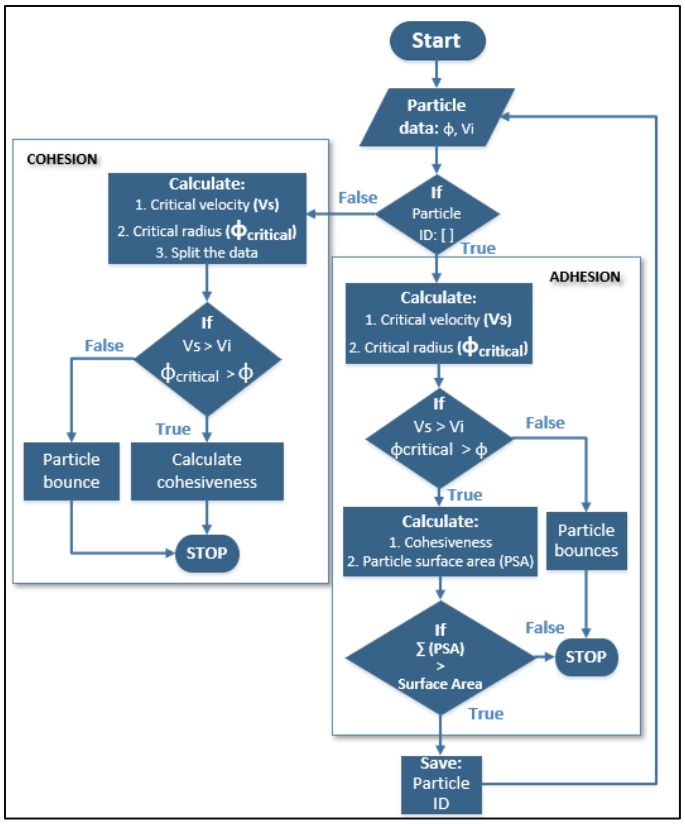


*Figure 2: Flowchart used to calculate the cohesiveness of snow*

impact velocity of the particle is equal to or less than the critical stick velocity [15]. This is the condition which explains critical stick velocity. Furthermore, Eidevåg [7] expands on this and gives a simplified version of the same:

$$V_s = \frac{3\sqrt{3}}{4} \times \sqrt{\frac{K_1}{\rho}} \left(\frac{\pi^2 W^5}{R^2 E^2}\right)^{\frac{1}{6}} \tag{7}$$

Here $K_1 \sim 0.9355$ is an integration constant, ρ is the density of the material, W is the work of adhesion/ cohesion between 2 subsequent layers. Interestingly in [7], a comparison of single-particle collisions and agglomerate collisions on surfaces, has been conducted using DEM simulations. This revealed the following: as the number of particles within an agglomerate increases, the maximum velocity at which the agglomerate sticks also increases. Additionally, the average stick velocity of agglomerates with 3 to 5 particles is approximately twice that of a single particle. A regression line, serving as an extrapolated approximation of potential agglomerate collisions with surfaces, was generated to estimate new stick velocities for particle agglomerates. Interactions are primarily driven by normal forces, with sliding and rolling models contributing to additional force and torque. To assess their impact, critical radii for rolling and sliding are introduced.

The critical radius for rolling ($R_{cr-roll}$) is defined as the particle radius at which rolling begins due to the moment generated by the particle's own weight. A linear momentum balance from the particle's center provides the governing relationship for this condition [7],

$$mgR_{cr-roll} = \frac{\pi W R_{cr-roll}\, a_0}{2}\left(\frac{\Delta\gamma}{\gamma}\right) \quad (8)$$

When the particle makes contact with an inclined surface (Fig. 3a) rather than a horizontal surface, then the moment ($M_c$) is a function of the angle the particle makes with the surface. Where $\Delta\gamma/\gamma$ is the adhesion hysteresis, and its value has been found to be equal to 1 [7], $a_0$ is the contact radius at equilibrium, $R_{cr-roll}$ is the critical radius for rolling. This requires the modification of equation (8) to include the angle $\theta$ in the calculation.

$$mg\sin\theta \times R_{cr-roll} = \frac{\pi W R_{cr-roll}\, a_0}{2}\left(\frac{\Delta\gamma}{\gamma}\right) \quad (9)$$

Further simplification results in this equation:

$$R_{cr-roll} = \left(\frac{3(6)^{\frac{2}{3}}}{16}\right)^{\frac{3}{7}}\left(\left(\frac{\pi W^4}{E^*}\right)^{\frac{1}{3}}\left(\frac{1}{\rho g\ \sin\theta}\right)\left(\frac{\Delta\gamma}{\gamma}\right)\right)^{\frac{3}{7}} \quad (10)$$

Similarly, the critical radius for sliding $R_{\mathrm{cr-slide}}$ is defined as the radius at which a particle begins to slide due to its own weight. The force balance governing this condition is given by [7]:

$$mg = F_{cs} = \mu_f|F_n + 2F_c| = 2\mu_f F_c \quad (11)$$

When this particle is on an inclined plane which makes θ degrees with the horizontal, the sliding force is expressed $F_S$ is:

$$F_S = mg \times \sin\theta = 2\mu_f F_c \quad (12)$$

$$R_{cr-slide} = \left(\frac{9\mu_f W}{4\rho g\ \sin\theta}\right)^{\frac{1}{3}} \quad (13)$$

Since the rolling moment and sliding force are not dimensionally homogeneous, a critical radius for rolling and sliding determines whether a particle stays on the surface or bounces off. When particles make contact, they possess a certain amount of gravitational potential energy, which can be calculated using [25]:

$$Gravitational\ potential\ energy = mgR \quad (14)$$

here, m is the mass of the particle and g is the acceleration due to gravity. Thus, a critical radius criterion has been established for inclined surfaces. Quantities that define flowability provide an estimate of the snow's cohesive and adhesive properties. The dimensionless numbers that describe the cohesion /stickiness of granular matter have been stated below:

Cohesion number [25]**:** The ratio of the work of cohesion to the particle's gravitational potential energy, considering a characteristic height is equal to the previously defined equivalent radius R.

$$Coh_{GPE} = \frac{Work\ of\ cohesion}{Gravitational\ potential\ energy} = \frac{7.09 \times \left(\frac{W^5 R^4}{E^2}\right)^{\frac{1}{3}}}{mgR} = \frac{1}{\rho g}\left(\frac{W^5}{E^2 R^8}\right)^{1/3} \quad (15)$$

Bond number [26] [27]**:** The cohesive granular Bond number is defined as the ratio of the attractive interparticle force $F_a$ to the particle's weight mg.

$$Bo = \frac{Adhesive\ force}{Weight\ of\ the\ particle} = \frac{F_a}{mg} = \frac{\frac{3}{2}\pi RW}{mg} \quad (16)$$

The sticking efficiency as defined by Makkonen in [9], is the ratio of particles that stick to the surface to the particles that collide with a given surface.

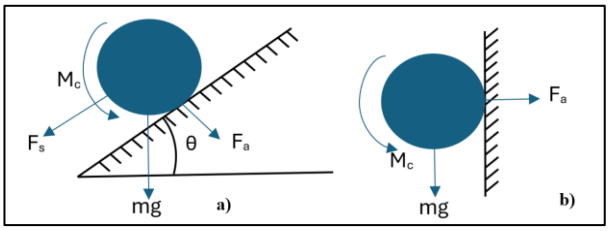


*Figure 3: Particle adhesion mechanism [7]*

## IV. Results & Conclusion:

### *A. Experimental*

From the various quantities that were measured during the tests- temperature, particle size, and particle fall velocity were considered for an adhesion/ cohesion-based prediction of particles that make contact with the surface. Fig. 4 compares particle diameter and velocity for three different temperature conditions. The data in Fig. 4 shows an inverse relationship between the average particle size in comparison to average particle fall velocity.

The graph in Fig. 5a presents the trend in normalized snow accumulation height as a function of surface inclination angle across different temperature conditions. The observed trend shows that as the surface angle increases, the accumulated snow height decreases, reinforcing the idea that steeper inclines lead to more snow displacement due to gravitational and impact forces. This behavior is expected, as snow particles are more likely to slide, bounce, or roll off rather than adhere to the surface when the inclination is greater.

From the experimental data, the only observed anomaly in Fig. 5a is regarding the snow accumulation height, at $-10℃$ remains consistent across all surfaces, regardless of incline angle. This unexpected behavior requires further investigation to identify potential influencing factors. Additionally, repeatability tests should be conducted to verify the reliability of these findings.

### *B. Numerical*

The numerical analysis of the experimental test data offers a glimpse into the properties of artificial snow under specific temperature conditions. Among these properties, the focus is on cohesiveness.

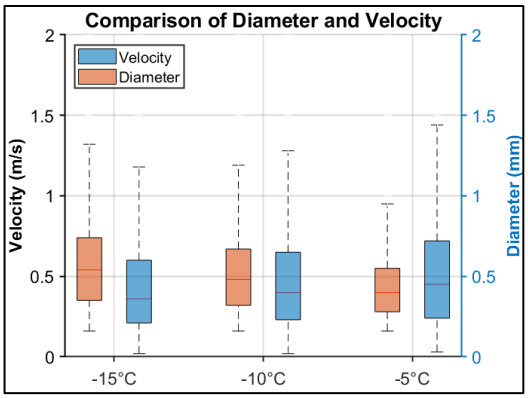


*Figure 4: Snow particle diameter and velocity measurements*

By analyzing particle data such as diameter and velocity from the experiments, it can be predicted whether a particle will stick or not. For particles predicted to stick, non-dimensional numbers that indicate their stickiness have been evaluated. Snow tends to be less cohesive or sticky at cold temperatures due to it being categorized as dry snow which lacks liquid water content.

Fig. 6 illustrates the distribution and average cohesion numbers, for a range of temperatures from the numerical results. The whiskers in the boxplot represent the full range of the data from the minimum to the maximum values providing insight into the overall spread of the dataset. The outliers have been ignored for ease of visualization. The green markers and accompanying lines represent the mean cohesion numbers in both plots in Fig. 6, which increase as temperatures rise. This suggests a clear trend: higher temperatures lead to stronger cohesion. The median cohesion number also consistently rises with temperature, reinforcing this pattern in Fig 6a. This is a similar trend that can be seen in Fig. 6b for the Bond number. Here, both dimensionless numbers explain the adhesiveness of snow as a function of temperature.

The data from the numerical model gives a normalised sticking efficiency of artificial snow on inclined surfaces. The results in Fig. 5b shows a clear trend: as the angle of the surface increases, the amount of snow accumulation decreases. This only backs up the claim that steeper surface slopes generally tends to have less snow accumulation.

Both the numerical sticking efficiency and experimentally obtained sticking efficiency follow a similar trend, showing decreasing snow accumulation with increasing surface incline, thereby reinforcing the accuracy of the numerical model. This consistency suggests that the computational model effectively captures the key physical mechanisms governing snow adhesion. However, some limitations remain, such as the degree of agreement between numerical and experimental values, which require further refinement for improved accuracy. Future research should include a detailed particle analysis to examine the morphology of snow, providing deeper insights into its structural characteristics.

Additionally, the effects of porosity on snow accumulation and adhesion should be investigated to establish a robust criterion for adhesion for agglomerates consisting of a large number of constituents, which in turn would improve the

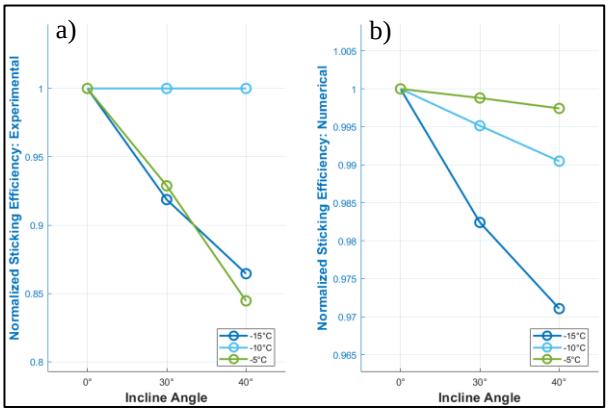


*Figure 5: Normalized sticking efficiency vs Surface incline*
*a) Experimental Sticking Efficiency b) Numerical Sticking Efficiency*

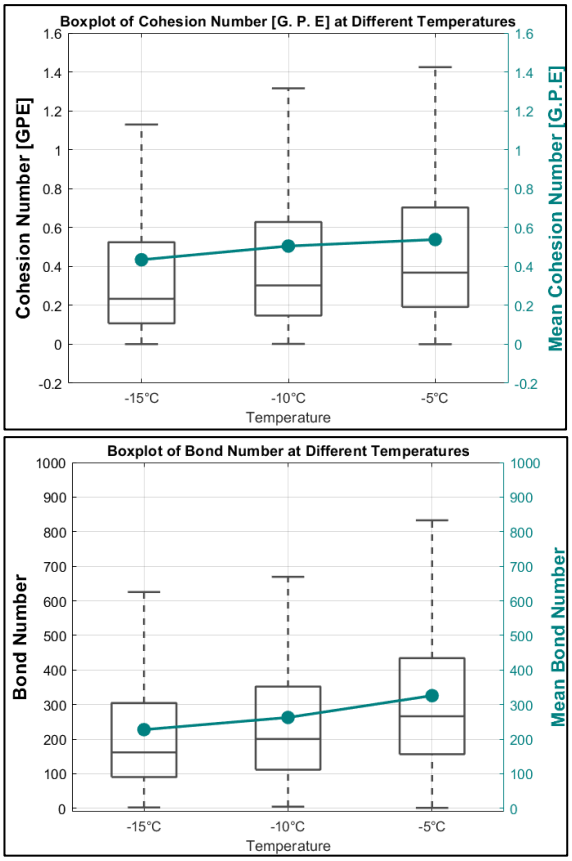


*Figure 6: Non dimensional numbers for different test cases.*
*(a) Cohesion number, (b) Bond number*

numerical accuracy. Further studies can explore adhesion and cohesion mechanisms across different surface materials, considering surface roughness and its influence on snow particle attachment. Understanding these factors will enhance predictive models and improve applications in snow management, infrastructure design, and artificial snow production.

## V. REFERENCES


[1] M. Carvalho *et al.*, "Towards a Model of Snow Accretion for Autonomous Vehicles," *Atmosphere 2024, Vol. 15, Page 548*, vol. 15, no. 5, p. 548, Apr. 2024, doi: 10.3390/ATMOS15050548.

[2] B. Mohammadian, M. Sarayloo, A. Abdelaal, A. Raiyan, D. K. Nims, and H. Sojoudi, "Experimental and Theoretical Studies of Wet Snow Accumulation on Inclined Cylindrical Surfaces," *Modelling and Simulation in Engineering*, vol. 2020, no. 1, p. 9594685, Jan. 2020, doi: 10.1155/2020/9594685.

[3] "The Snowflake - Kenneth Libbrecht - Google Books." Accessed: Feb. 14, 2025. [Online]. Available: https://books.google.ca/books?hl=en&lr=&id=ZRcSEAAAQBAJ&oi=fnd&pg=PP1&dq=Libbrecht,+Kenneth.+The+snowflake+google+scholar&ots=_zHpWjTFxx&sig=nmyjrfuVCcjpQGy1wpZo_Td3YRg#v=onepage&q=Libbrecht%2C%20Kenneth.%20The%20snowflake%20google%20scholar&f=false

[4] E. Villeneuve, C. Charpentier, J. D. Brassard, G. Momen, and A. Lacroix, "Aircraft Anti-Icing Fluids Endurance Under Natural and Artificial Snow: a Comparative Study," *International Review of Aerospace Engineering*, vol. 15, no. 1, pp. 1–11, 2022, doi: 10.15866/IREASE.V15I1.21324.

[5] X. Jiang, H. Cui, Z. Mo, and S. Guo, "Experimental Study on the Characteristics of Wind-Induced Snow Distribution on Structures with Openings," *Symmetry 2025, Vol. 17, Page 249*, vol. 17, no. 2, p. 249, Feb. 2025, doi: 10.3390/SYM17020249.

[6] M. Liu, Q. Zhang, F. Fan, and S. Shen, "Experiments on natural snow distribution around simplified building models based on open air snow-wind combined experimental facility," *Journal of Wind Engineering and Industrial Aerodynamics*, vol. 173, pp. 1–13, Feb. 2018, doi: 10.1016/J.JWEIA.2017.12.010.

[7] T. Eidevåg, P. Abrahamsson, M. Eng, and A. Rasmuson, "Modeling of dry snow adhesion during normal impact with surfaces," *Powder Technol*, vol. 361, pp. 1081–1092, Feb. 2020, doi: 10.1016/J.POWTEC.2019.10.085.

[8] T. Eidevåg, E. S. Thomson, S. Sollén, J. Casselgren, and A. Rasmuson, "Collisional damping of spherical ice particles," *Powder Technol*, vol. 383, pp. 318–327, May 2021, doi: 10.1016/J.POWTEC.2021.01.025.

[9] L. Makkonen, "Models for the growth of rime, glaze, icicles and wet snow on structures," *Philosophical Transactions of the Royal Society A: Mathematical, Physical and Engineering Sciences*, vol. 358, no. 1776, pp. 2913–2939, 2000, doi: 10.1098/RSTA.2000.0690.

[10] B. Gerling, H. Löwe, and A. van Herwijnen, "Measuring the Elastic Modulus of Snow," *Geophys Res Lett*, vol. 44, no. 21, pp. 11,088-11,096, Nov. 2017, doi: 10.1002/2017GL075110.

[11] A. Wautier, C. Geindreau, and F. Flin, "Linking snow microstructure to its macroscopic elastic stiffness tensor: A numerical homogenization method and its application to 3-D images from X-ray tomography," *Geophys Res Lett*, vol. 42, no. 19, pp. 8031–8041, Oct. 2015, doi: 10.1002/2015GL065227.

[12] A. Sheet, "PLEXIGLAS ® GENERAL INFORMATION AND PHYSICAL PROPERTIES PLEXIGLAS ® Acrylic Sheet".

[13] J. P. Morrissey, S. Thakur, and J. Y. Ooi, "EDEM Contact Model: Adhesive Elasto-Plastic Model," 2014, doi: 10.13140/RG.2.2.10139.18724.

[14] J. Olsson, "Surface impact of wet and dry agglomerates," 2017. Accessed: Feb. 12, 2025. [Online]. Available: https://hdl.handle.net/20.500.12380/251825

[15] C. Thornton, "Granular Dynamics, Contact Mechanics and Particle System Simulations: A DEM study," *Granular Dynamics, Contact Mechanics and Particle System Simulations: A DEM study*, vol. 24, pp. 1–195, Sep. 2015, doi: 10.1007/978-3-319-18711-2/COVER.

[16] J. N. Israelachvili, "Intermolecular and Surface Forces, Third Edition," *Intermolecular and Surface Forces, Third Edition*, pp. 1–674, Jan. 2010, doi: 10.1016/C2009-0-21560-1.

[17] M. Soltani and G. Ahmadi, "On particle adhesion and removal mechanisms in turbulent flows," *J Adhes Sci Technol*, vol. 8, no. 7, pp. 763–785, 1994, doi: 10.1163/156856194X00799.

[18] D. TABOR, "Surface Forces and Surface Interactions," *Plenary and Invited Lectures*, pp. 3–14, Jan. 1977, doi: 10.1016/B978-0-12-404501-9.50009-2.

[19] F. M. Fowkes, "ATTRACTIVE FORCES AT INTERFACES," *Ind Eng Chem*, vol. 56, no. 12, pp. 40–52, Dec. 2002, doi: 10.1021/IE50660A008.

[20] F. London, "The general theory of molecular forces," *Transactions of the Faraday Society*, vol. 33, pp. 8–26, 1937, doi: 10.1039/TF937330008B.

[21] J. Kloubek, "Calculation of surface free energy components of ice according to its wettability by water, chlorobenzene, and carbon disulfide," *J Colloid Interface Sci*, vol. 46, no. 2, pp. 185–190, Feb. 1974, doi: 10.1016/0021-9797(74)90001-0.

[22] W. M. Ketcham and P. V. Hobbs, "An experimental determination of the surface energies of ice," *Philosophical Magazine*, vol. 19, no. 162, pp. 1161–1173, 1969, doi: 10.1080/14786436908228641.

[23] "(PDF) Surface properties of PMMA films with different molecular weights." Accessed: Feb. 05, 2025. [Online]. Available: https://www.researchgate.net/publication/259759652_Surface_properties_of_PMMA_films_with_different_molecular_weights

[24] C. Ozean and N. Hasirci, "Evaluation of surface free energy for PMMA films," *J Appl Polym Sci*, vol. 108, no. 1, pp. 438–446, Apr. 2008, doi: 10.1002/APP.27687.

[25] M. A. Behjani, N. Rahmanian, N. Fardina bt Abdul Ghani, and A. Hassanpour, "An investigation on process of seeded granulation in a continuous drum granulator using DEM," *Advanced Powder Technology*, vol. 28, no. 10, pp. 2456–2464, Oct. 2017, doi: 10.1016/J.APT.2017.02.011.

[26] A. Castellanos, "The relationship between attractive interparticle forces and bulk behaviour in dry and uncharged fine powders," *Adv Phys*, vol. 54, no. 4, pp. 263–376, Jun. 2005, doi: 10.1080/17461390500402657.

[27] M. Capece, R. Ho, J. Strong, and P. Gao, "Prediction of powder flow performance using a multi-component granular Bond number," *Powder Technol*, vol. 286, pp. 561–571, Dec. 2015, doi: 10.1016/J.POWTEC.2015.08.031.